Nano Research

Open Access

Review Article

Research progress on alkaline anion exchange membranes (AEMs) for the application of hydrogen production by water electrolysis

Qichen Lu[1] ✉, Xupeng Yan[1], Weiqi Guo[1], Guangshan Li[2], Jinyi Wang[1], Nan Jiang[2], Xiaolong Wang[1], Teer Ba[3], Peng Liu[1], Jianing Zhou[2], Ju Wang[1], Lin Hu[1], Tianyi Zhou[1], Ruling Huang[1], Bo Hu[1], Kexin Zhang[1], and Zhibo Ren[1] ✉

[1] *Huaneng Clean Energy Research Institute, Beijing 102209, China*
[2] *Yimin Power Plant, Hulunbuir 021134, China*
[3] *Huaneng Inner Mongolia Eastern Energy Co., Ltd., Hailar 021000, China*

Cite this article: *Nano Research*, **2025**, *18*, 94907252. https://doi.org/10.26599/NR.2025.94907252

ABSTRACT: The alkaline anion exchange membrane (AEM) water electrolysis technology has advantages of low cost, high current density, and fast dynamic response, and it has attracted more attention from researchers in the last few years. As one of the core components in this water electrolysis technology, AEMs play a crucial role in improving the hydrogen production efficiency of electrolyzers. However, it is difficult to achieve high ionic conductivity and high alkaline stability of AEMs simultaneously, which limits the practical applications of this hydrogen production technology. This review focuses on alkaline AEMs, which can be applied in the field of water electrolysis. Firstly, the performance evaluation system and the structure–activity relationship of AEMs are proposed. Then, the research progress of AEMs for water electrolysis was illustrated in detail. Finally, the current challenges and outlooks for development of AEMs applied in water electrolysis are presented. We hope this review can provide a new perspective for the design and preparation of AEMs for the demand of practical applications in water electrolysis.

KEYWORDS: anion exchange membranes, water electrolysis, green hydrogen, performance evaluation system

1 Introduction

Against the backdrop of global carbon neutrality, hydrogen energy is a potential key carrier for energy transition, and it is gaining unprecedented global consensus. Hydrogen production by water electrolysis (WE) using renewable energy electricity, like wind and photovoltaic power generation, has a potential to transfer a large amount of renewable energy electricity to the fields which are difficult to deeply decarbonize, making it a key direction for global energy enterprises and research institutions to focus on technological research and industrial layout [1–3]. According to the types of electrolytes, hydrogen production technology through water electrolysis can be mainly divided into four categories: alkaline water electrolysis [4, 5], proton exchange membrane (PEM) water electrolysis [6, 7], solid oxide electrolysis cell (SOEC) water electrolysis [8, 9], and anion exchange membrane (AEM) water electrolysis [10, 11]. At present, the most mature technology is the alkaline WE technology, which only applies non-precious metal materials for catalysts, which has a relatively low cost and large-scale commercial application [12, 13]. PEMWE technology has advantages of high current density and fast dynamic response, however, it faces significant economic challenges due to the substantial costs associated with membranes and precious metal catalysts [14–17]. SOEC technology has a low power consumption for hydrogen production, but its operating temperature needs to exceed 700 °C, which limits its scope of application scenarios [8, 18]. With the continuous expansion of installation scale of new energy power, these existing hydrogen production technologies, such as alkaline WE, PEMWE, and SOEC, cannot feed the demand in the field of large-scale renewable energy water electrolysis. Recently, AEMWE technology [19–22] has become a key direction for technological breakthroughs in hydrogen production field, which combines the advantages of traditional alkaline WE and PEMWE. On the one hand, it can use low-cost material systems [23, 24], and on the other hand, it can use solid electrolytes to achieve high current density and fast dynamic response [15].

AEMs are the key components in various electrochemical reactors, including water electrolyzers [25], fuel cells [26], CO_2 reduction electrolyzers [27, 28], N_2 reduction electrolyzers [29], and

Received: November 19, 2024; **Revised:** January 10, 2025
Accepted: January 13, 2025

✉Address correspondence to Qichen Lu, qc_lu@qny.chng.com.cn; Zhibo Ren, zb_ren@qny.chng.com.cn

batteries [30]. In the case of water electrolyzers, AEMs play an important role in conducting OH^-, separating hydrogen and oxygen gases, and blocking the direct transfer of electrons between two electrodes during the WE process [31, 32]. In the structure of AEMs, ion transport is achieved through the electrostatic interaction between the functional groups and the anions in the solution [33, 34]. However, due to the lower mobility of OH^- compared with H^+, the ion conductivity of AEMs is lower than that of PEMs [35], which increases the energy consumption of hydrogen production in WE. Although increasing the concentration of functional groups can improve the ion conductivity of AEMs, it can also cause an increase in water uptake and swelling ratio and reduce the mechanical properties and dimensional stability [36–38]. Meanwhile, high concentrations of functional groups can also increase the contact between polymers and OH^-, reducing the alkaline stability of AEMs [39]. Therefore, achieving an excellent comprehensive performance of AEMs, which has high ion conductivity, high alkali and dimensional stability, and high mechanical properties, is a key technical obstacle restricting the industrial application of AEMWE for hydrogen production.

In this review, we will summarize the research progress of the alkaline AEMs for the application of hydrogen production through water electrolysis. We first propose on the performance evaluation system and the structure–activity relationship of AEMs, mainly including ionic exchange capacity (IEC), ionic conductivity, chemical stability, dimensional stability, mechanical strength, and hydrogen permeability. Then, we illustrate the research progress of AEMs for the applications of water electrolysis in detail. Finally, we summarize the current status and challenges of AEMs for hydrogen production by water electrolysis and present an outlook on the development of AEMs in future. We hope this review can provide a new perspective for the design and preparation of AEMs for the demand of practical applications in water electrolysis.

2 Performance evaluation of AEMs

The molecular structure of AEMs mainly contains polymer skeleton and cationic groups. Polymer skeleton plays an important role in maintaining the overall structure of the membrane, while cationic groups are used to conduct anions as functional groups. The structure of AEMs is closely related to their intrinsic performance, and the performance evaluation system of AEMs mainly includes the following aspects: ionic exchange capacity, ionic conductivity, chemical stability, dimensional stability, mechanical strength, and hydrogen permeability (Fig. 1). In this part, we will illustrate the performance evaluations system of AEMs and further elaborate on their structure–activity relationship.

2.1 Ionic exchange capacity

Ionic exchange capacity represents the content of functional groups in AEMs. Generally, with the increase of IEC value, the concentration of functional groups will increase, which is more conducive to improving ionic conductivity. However, high IEC will lead to the decrease of alkaline resistance stability and dimensional stability. Therefore, it is necessary to have an appropriate IEC for AEMs to achieve better comprehensive performance in practical applications.

2.2 Ionic conductivity

Ionic conductivity is a critical factor for evaluating the performance of AEMs, which reflects the anion transport ability of AEMs and directly affects the hydrogen production efficiency of electrolyzers. The common method to improve the ionic conductivity of AEMs is increasing the IEC, but it will cause a decrease in stability as discussed above, which will affect the stable operation of the electrolyzers. In addition, optimizing the molecular structure of AEMs can improve the internal microphase separation structure, which can achieve an increase in ionic conductivity as well as maintain chemical and dimensional stability.

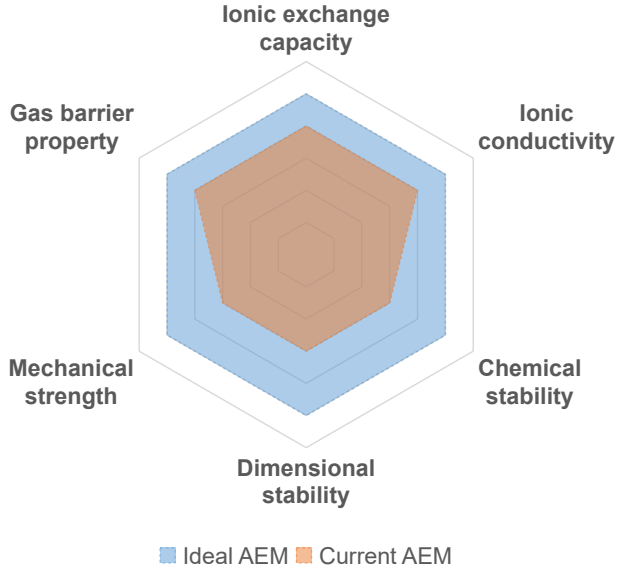

Figure 1 The performance evaluation system of AEMs for water electrolysis.

2.3 Chemical stability

Chemical stability is another key factor for evaluating the performance of AEMs. AEM electrolyzers usually work at an environment of high-temperature alkaline solutions, thus AEMs need to possess excellent alkaline and thermal stability, which can ensure the stability of electrolyzers. The alkaline stability is closely related to the structure of polymer skeleton and cationic groups in AEMs. Although AEMs with polymer skeleton structure of poly (arylene ether) have been studied earlier and have obvious advantages on the cost, the ether bonds in the skeleton structure are easily attacked by OH^- [40] (Fig. 2), and the degradation of the skeleton structure will lead to the poor alkaline stability. Recently, researchers have designed the AEMs containing poly aryl skeleton structure without ether bonds, which improved the alkaline resistance of AEMs.

In terms of the alkaline resistance of cationic groups, Lee et al. proposed that under alkaline conditions, AEMs containing quaternary ammonium cations are prone to nucleophilic substitution and Hofmann elimination reactions, resulting in poor chemical stability (Fig. 3). To further study the effects of the cationic groups' structure on the alkaline stability of AEMs, Marino et al. [41] compared the half-life of different types of quaternary ammonium cations in 6 M NaOH aqueous solution at 160 °C using tetramethyl ammonium (TMA) as a benchmark (Table 1). The 6-azonia-spiro[5.5]undecane (ASU) and N,N-dimethylpiperidinium (DMP) exhibited higher alkaline stability than TMA, which is due to reducing the possibility of nucleophilic substitution and Hofmann elimination reactions induced by the stable hexagonal ring structure in ASU and DMP.

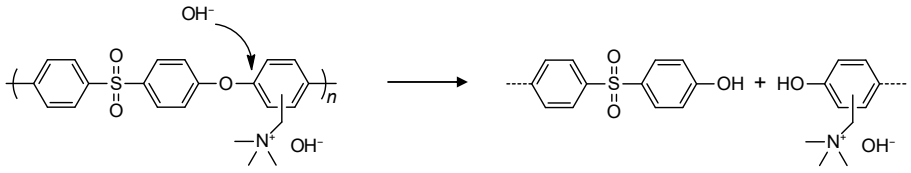

Figure 2 The degradation pathway of poly (arylene ether) backbones structure in alkaline solution.

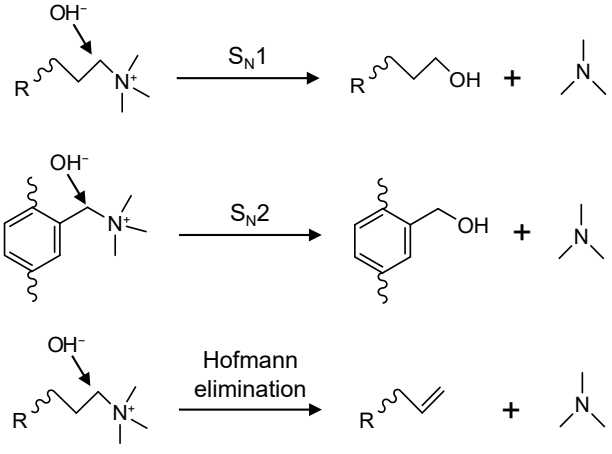

Figure 3 The degradation pathways of quaternary ammonium cations in alkaline solution. S_N1: unimolecular nucleophilic substitution reaction and S_N2: bimolecular nucleophilic substitution reaction.

Table 1 Comparisons of alkaline resistance of different quaternary ammonium cations at 160 °C in 6 M NaOH [41]

Quaternary ammonium cations	Abbreviation	Half-life (h)
	ASU	110
	DMP	87.3
	DMPy	37.1
	ASN	28.4
	TPA	7.19
	BMP	7.26
	TMA	61.9
	MAABCO	13.5
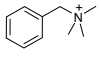	BTM	4.18
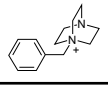	BAABCO	1.38

2.4 Dimensional stability

The evaluation for dimensional stability of AEMs mainly includes the water uptake and swelling ratio. If the dimensional stability of AEMs is poor, volume expansion will occur during the operation of the electrolyzers, which easily causes the separation between AEMs and coated catalyst layers; meanwhile, during the shutdown period, AEMs will shrink and generate mechanical stress, which affects the long-term operation of electrolyzers. Constructing crosslinked network is an efficient strategy to enhance the dimensional stability of AEMs. Li et al. [42] prepared various crosslinked AEMs based on high ion conductive poly(vinyl benzyl methylpyrrolidinium) and rigid polysulfone (PSF), using different diamine structures as crosslinked agents (Fig. 4). The crosslinked AEMs exhibited excellent resistance to free radical chemistry and moderate ionic conductivity, while its dimensional and alkaline stability were also improved.

2.5 Mechanical strength

Mechanical strength mainly includes tensile strength and elongation at break. Excellent mechanical strength can ensure the integrity of AEMs during the hydrogen production process and avoid the mixture of hydrogen and oxygen to ensure the safe operation of electrolyzers. Han et al. [43] designed an AEM structure of multi-cation cross-linked poly(2,6-dimethylphenylene oxide) (PPO) (*x*(QH)*n*QPPO; QPPO: quaternized PPO). The flexible cross-linked agent containing multiple cations overcomes the disadvantages of increased membrane brittleness and decreased ionic conductivity using conventional cross-linked agents, and it could improve the tensile strength, elongation at break, as well as ionic conductivity of AEMs.

2.6 Gas barrier performance

Gas barrier performance of AEMs is also an important factor for the safe operation of electrolyzers, and it is usually evaluated by hydrogen permeability for water electrolysis. Low hydrogen permeability can prevent the hydrogen produced in the cathode side from penetrating into the anode side to avoid the mix of hydrogen and oxygen. In practical application process, the requirement for hydrogen permeability of electrolyzers can be met by increasing the thickness of AEMs.

Recently, a series of target performance values for AEMs were proposed in the European Union (EU) "Horizon 2020" project, which is listed in Table 2 [40]. These target performance parameters can be regarded as reference values for the evaluation of AEMs for the applications of water electrolysis.

3 Applications of AEMs in water electrolysis

AEMs are the key component in the electrolyzers for AEMWE, thus, it is necessary to use AEMs with excellent comprehensive performance to ensure the long-term and efficient operation of electrolyzers. In 2012, Xiao et al. [44] first applied self-crosslinking quaternary ammonia polysulfone AEM for hydrogen production by water electrolysis, and they used Ni-Fe catalyst as an anode and Ni-Mo catalyst as a cathode. The current density of the cell was about 400 mA·cm^{-2}@1.8 V under pure water conditions of 70 °C, and this electrolysis cell could continuously operate for 8 h at this

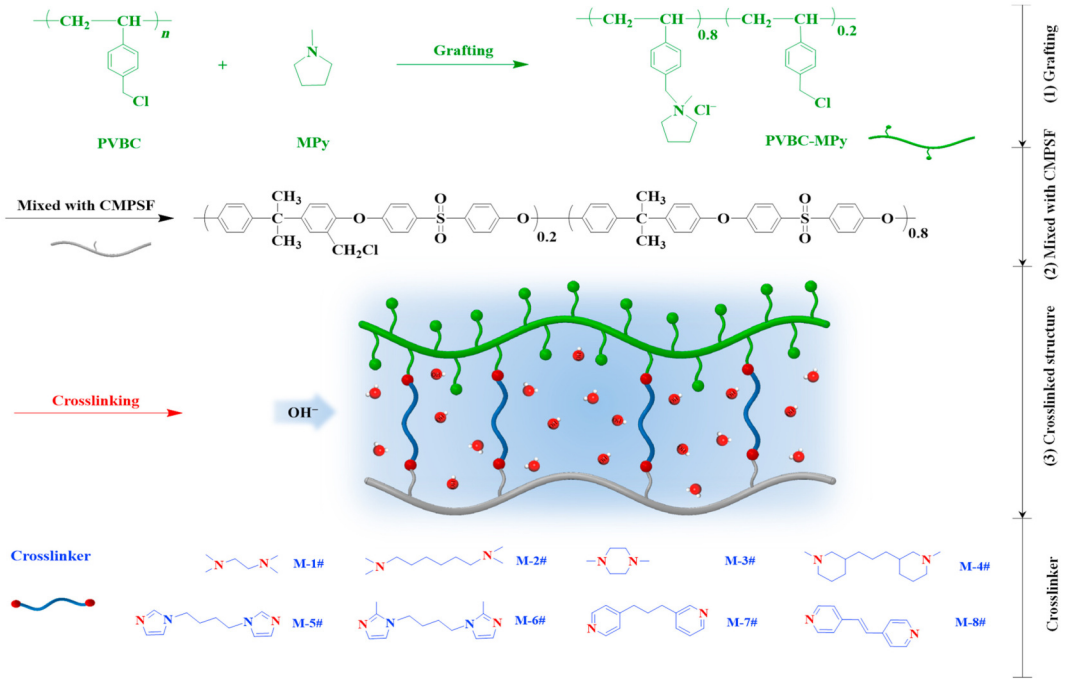

Figure 4 The schematic synthesis process of various cross-linked AEMs. Reproduced with permission from Ref. [42], © Elsevier B.V. 2021.

Table 2 The target performance values for AEMs proposed in the EU "Horizon 2020" project [40]

Parameter	Target value
Ionic conductivity	> 50 mS·cm^{-1} (at room temperature)
Chemical stability	> 2000 h real or simulated operation in an electrolyzer
Dimensional stability	≤ 1% in machine direction≤ 4% in transverse direction
Tensile strength	> 15 MPa
Elongation at break	> 100%

current density (Fig. 5). Due to the unique advantages of this hydrogen production technology, researchers began to apply AEMs in the field of hydrogen production by water electrolysis.

3.1 Poly (arylene ether)-type AEMs

Poly (arylene ether)-type AEMs were mainly prepared by grafting cationic groups onto the poly (arylene ether) skeleton, and they have advantages of simple preparation process, low cost, good film-forming and flexibility. Thus, this type of AEM received widespread attention in the early stage of AEM research, and was also first applied in water electrolysis [44].

Parrondo et al. [45] grafted different quaternary ammonium or imidazole groups onto the polysulfone skeleton, and this prepared AEM could be applied for water electrolysis (Fig. 6). Thereinto, the PSF-TMA$^+$ AEM with a terminal trimethylammonium structure showed the best electrochemical performance, with a current density of 400 mA·cm^{-2}@1.8 V at 50 °C using pure water as a feed. It is worth noting that, in the second and third polarization curve tests, a significant performance degradation could be observed, which is caused by the dissolution of CO_2. Meanwhile, the performance degradation of the electrolysis cell during long-term testing was induced by the poor alkaline stability of polysulfone structure.

Cross-linking strategy is an effective way to improve the performance of AEM. By utilizing the functional groups at both ends of the crosslinking agent to combine with the main chain of the polymer, an AEM with a crosslinked network structure can be formed. An et al. [46] designed cross-linked polysulfone-based AEMs (chloromethylated polysulfone (CMPSF)) using three types of cross linkers, including 4,4'-trimethylenebis(1-methyl-piperidine) (BMP), N,N,N',N'-tetramethyl-1,6-diaminohexane (TMHDA), and 1,4-diazabicyclo [2.2.2]octane (DABCO) (Fig. 7). Among all the three AEMs, BMP-c-CMPSF membrane exhibited the highest

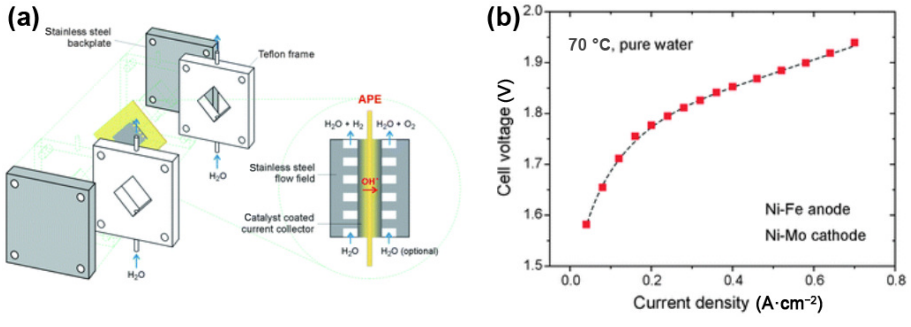

Figure 5 (a) Schematic illustration of an implementation of AEMWE. (b) Polarization curves of the AEMWE system based self-crosslinking quaternary ammonia polysulfone AEM in Ref. [44]. Reproduced with permission from Ref. [44], © The Royal Society of Chemistry 2012.

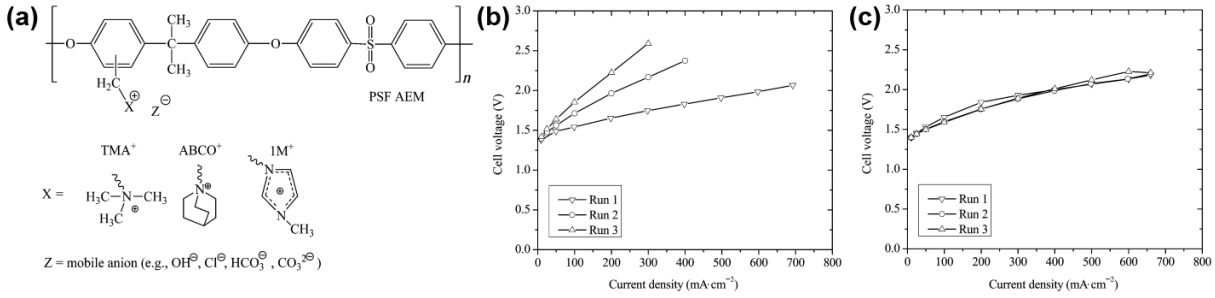

Figure 6 (a) The structure of grafted polysulfone skeleton AEMs. ((b) and (c)) Polarization curves of the AEMWE system based PSF-TMA$^+$ AEM (b) before and (c) after minimizing CO_2 exposure. Reproduced with permission from Ref. [45], © The Royal Society of Chemistry 2014.

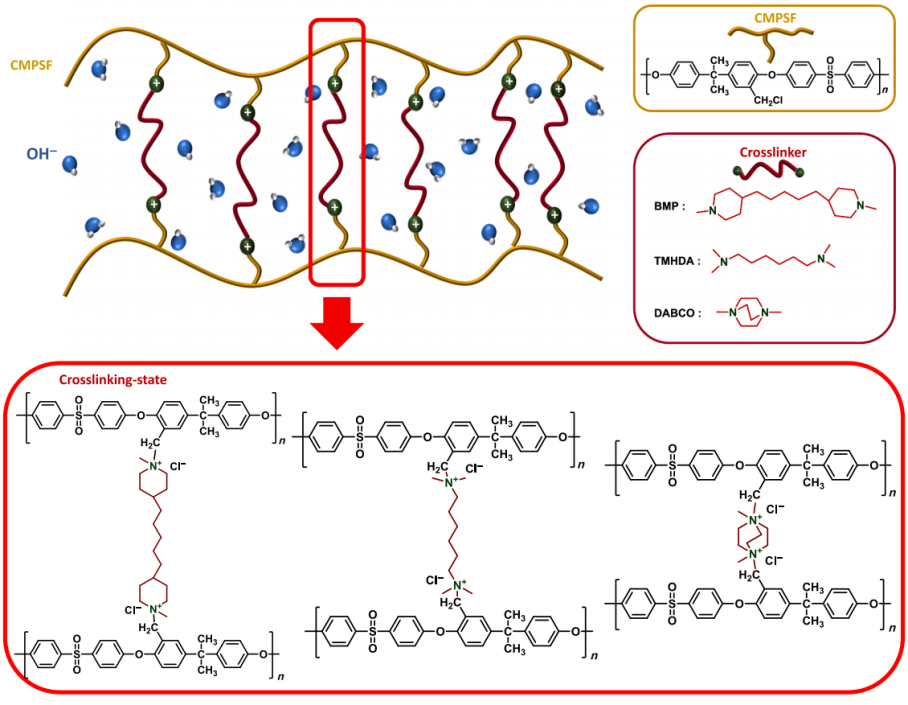

Figure 7 The structure of cross-linked polysulfone-based AEMs (CMPSF). Reproduced with permission from Ref. [46], © Elsevier Ltd. 2024.

properties with an IEC value of 1.58 mmol·g^{-1}, ionic conductivity of 53.7 mS·cm^{-1}, water uptake of 50%, and swelling ratio of 23%. After assembling the BMP-c-CMPSF membrane into electrolytic cell, the current density could reach 0.38 A·cm^{-2}@1.8 V.

Although the poly (arylene ether)-type AEMs have various advantages, the ether bonds were easily to be attacked by OH^-, which leads to the degradation of the skeleton structure [40] (Fig. 2), and results in the poor stability of this type of AEM applied for water electrolysis.

3.2 Polyolefin-type AEMs

Polyolefin is a common polymer skeleton without ether bonds, and the polyolefin-type AEMs could be constructed by simply modifying cationic groups onto the side chains, which has the characteristics of simple preparation process, low cost, and high ion transport performance.

Su et al. [47] prepared a series of piperidinium functionalized styrene–ethylene–butylene–styrene (SEBS) AEMs (SEBS-Pi) (Fig. 8), and the SEBS-Pi-73% showed the highest OH^- conductivity, which exceeded 10 mS·cm^{-1} at 30 °C. Meanwhile, this SEBS-Pi AEM exhibited excellent thermal stability, mechanical properties, and alkaline stability. After soaking into 1 M KOH solution at 80 °C for 576 h, the IEC and ionic conductivity of the SEBS-Pi AEM maintained high retention values. SEBS-Pi material was used as an ionic exchange membrane and ionomer in electrolysis cell, and the current density can reach 400 mA·cm^{-2}@2 V at 50 °C using a 5.6 wt.% KOH solution as the electrolyte. The continuous operation at the current density of 400 mA·cm^{-2} for 105 h only resulted in a voltage increase of 80 mV, demonstrating the stable electrochemical performance of the assembled cell.

Park et al. [48] prepared a series of mixed AEMs by blending poly(1-vinyl-3-imidazole-co-styrene) (PIS) and polyvinyl alcohol (PVA). The introduction of PVA could improve the film-forming ability and mechanical performance of the AEMs, as well as improve the OH^- conductivity. The PISPVA46 AEM exhibited the OH^- conductivity of 89.7 mS·cm^{-1} at 60 °C, which was gradually increased and reached the highest value after soaking in a 6 M KOH solution for 24 h. However, the OH^- conductivity would decrease by 56.2% after soaking for 240 h. As a result, the electrolyzer using PISPVA46 as a membrane could reach a current density of 547.7 mA·cm^{-2}@2.0 V under the condition of 0.5 M KOH at 60 °C, and the current density would decrease 21% after an 80 h continuous operation at 1.8 V cell voltage.

Polyolefin-type AEMs usually showed an improved alkaline

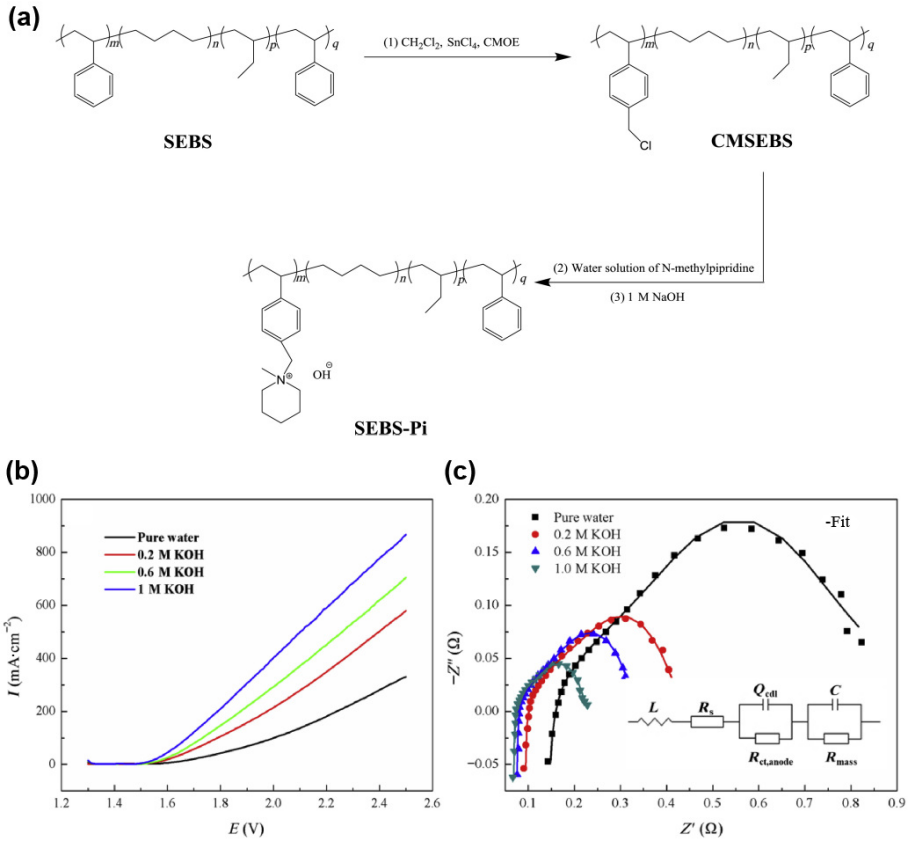

Figure 8 (a) The synthesis process of SEBS-Pi in Ref. [47]. (b) Polarization curves of the AEMWE system based SEBS-Pi AEM. (c) Impedance curves at 1.8 V. Reproduced with permission from Ref. [47], © Elsevier B.V. 2019.

resistance compared with poly (arylene ether)-type AEMs, however, they were prone to occur SN_2 reaction due to the formation of benzyl ammonium structure when introducing cationic groups in polyolefin skeleton [39] (Fig. 3), which leads to a degradation of cationic groups under alkaline conditions. In addition, the poor tensile strength of this type of AEM also limits their practical applications in electrolyzers.

3.3 Polyaryl-type AEMs

Polyaryl-type AEMs also have the skeleton structure without ether bonds, and due to the high rigid feature of this type of skeleton structure, polyaryl-type AEMs exhibit excellent mechanical strength and dimensional stability. Meanwhile, polyaryl-type AEMs show high ionic conductivity and alkaline stability, thus, this type of AEMs has attracted more and more attention in the field of water electrolysis in the past few years.

Cationic grafting based on the polyaryl backbone is the most traditional structural design method. Park et al. [49] prepared BPN1-100 and TPN1-100 AEMs by modifying terminal quaternary ammonium groups onto the flexible side chains of the polyaryl skeleton (Fig. 9). Both of the AEMs showed high OH^- conductivity (122 and 112 mS·cm^{-1} at 80 °C, respectively) and excellent alkaline stability. After soaking in 95 °C and 1 M KOH for 60 days, the structure of the AEMs remained intact, and the IEC of TPN1-100 membrane had nearly no decay. As for dimensional stability, BPN1-100 and TPN1-100 AEMs in OH^- form showed a swelling ratio of 66% and 23% at 80 °C, respectively. BPN1-100 and TPN1-100 had excellent electrochemical activity after assembled into electrolyzers. Using pure water as a feed at 50 °C, the BPN1-100 membrane could achieve a current density of 400 mA·cm^{-2} at 2.1 V, while the TPN1-100 membrane needs to increase the cell voltage by 0.25 V to reach the same current density.

Cha et al. [50] prepared quaternized polycarbazole (QPC-TMA) AEMs, which could achieve an OH^- conductivity of 154 mS·cm^{-1} at 80 °C (Fig. 10). After soaking in 1 M KOH solution at 80 °C for 1000 h, the IEC and OH^- conductivity were nearly unchanged. This QPC-TMA membrane could be used for water electrolysis, with a current density of 3.5 A·cm^{-2}@1.9 V. This water electrolysis performance was close to that of previously reported PEMWE technology. However, under the conditions of 1 M KOH electrolyte and 70 °C, the current density decreased by nearly 50% after a 10,000 s constant voltage testing at 1.6 V, indicating that its stability needs to be further improved.

Soni et al. [51] applied a grafted poly(fluorene-alt-tetrafluorobenzene) (PFOTFPh-TMA) AEM to an electrolysis cell (Fig. 11). This PFOTFPh-TMA AEM exhibited OH^- conductivity of over 100 mS·cm^{-1} at 80 °C, and the current density could reach 1.0 A·cm^{-2} at the cell voltage of 1.77 V under the conditions of 1 M KOH electrolyte and 80 °C, and the cell voltage increased by 50 mV after a 135 h operation at the current density of 0.2 A·cm^{-2}. After replacing the feed electrolyte with pure water, the applied voltage was only 1.94 V to reach the current density of 1.0 A·cm^{-2} and increased by 270 mV after a 120 h operation at the current density of 0.2 A·cm^{-2}.

In addition to the method of side-chain grafting, using N-methyl piperidine ketone and phenyl molecules as reactants, the piperidine cations can be directly connected to the polymer backbone structure through superacid condensation reaction. Yan et al. [52]

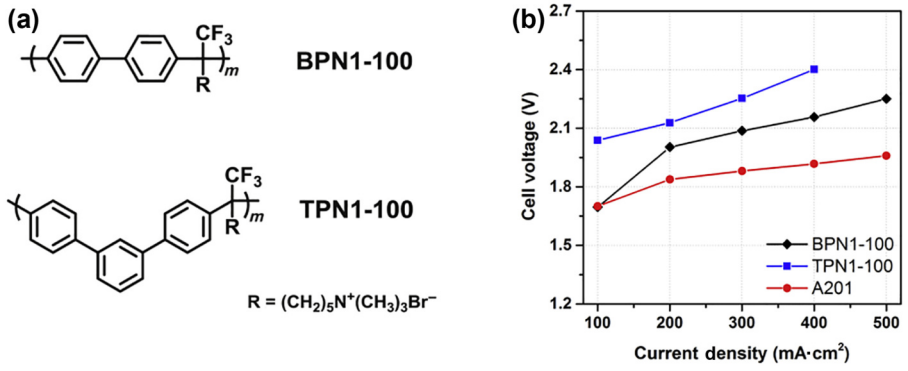

Figure 9 (a) The structure of BPN1-100 and TPN1-100 AEMs. (b) Polarization curves of the AEMWE system based BPN1-100 and TPN1-100 AEMs. Reproduced with permission from Ref. [49], © Elsevier B.V. 2017.

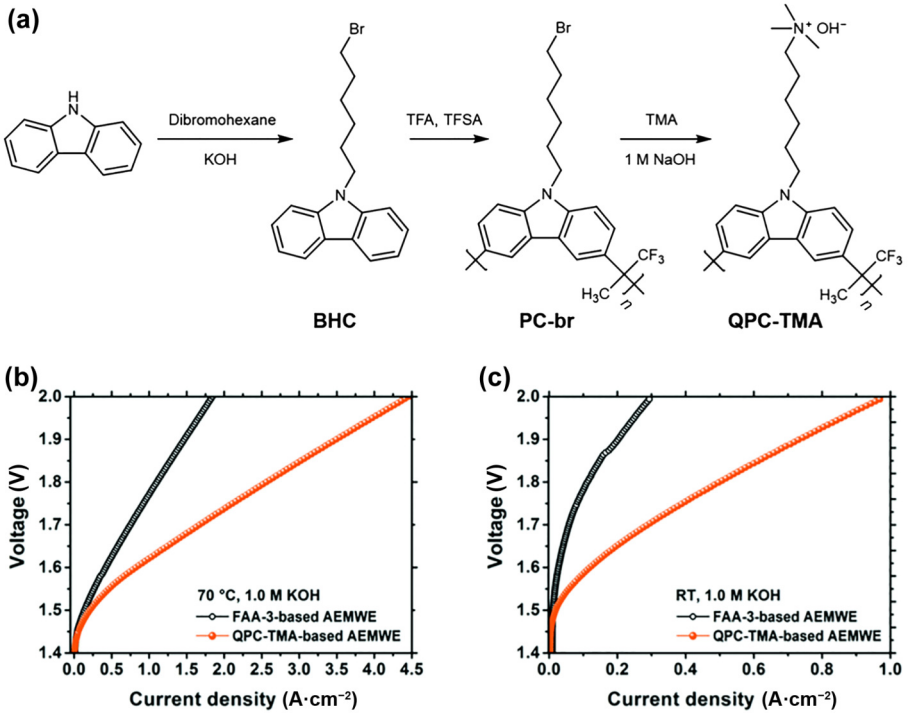

Figure 10 (a) The synthesis process of QPC-TMA in Ref. [50]. ((b) and (c)) Polarization curves of the AEMWE system based QPC-TMA AEM at different temperatures. Reproduced with permission from Ref. [50], © The Royal Society of Chemistry 2020.

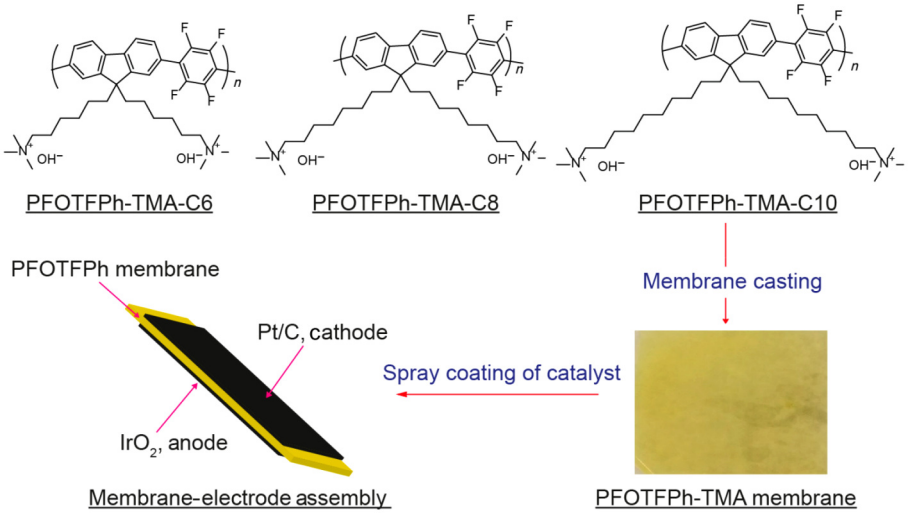

Figure 11 The structure of PFOTFPh-TMA AEMs. Reproduced with permission from Ref. [51], © American Chemical Society 2020.

prepared a quaternary ammonium functionalized poly(M-terphenyl-co-N-methyl-piperidine) (QMter-co-Mpi) membrane with a twisted skeleton structure using the m-triphenyl and N-methyl-4-piperidone as feedstocks (Fig. 12). The introduction of m-triphenyl with three-dimensional twisted structure in skeleton facilitated to constructing ionic transport channels inside the membrane. The OH^- conductivity of this QMter-co-Mpi membrane was 37 $mS{\cdot}cm^{-1}$ at 30 °C, and the IEC and OH^- conductivity could be retained by more than 80% after soaking in alkaline solution for 1000 h. When applying QMter-co-Mpi membrane in the electrolyzer, the current density could reach 1064 $mA{\cdot}cm^{-2}$@2.5 V at the condition of 50 °C and 1 $mol{\cdot}L^{-1}$ KOH feed solution, and the electrolyzer could achieve a stable electrolysis process for over 500 h at a cell voltage of 2.1 V under the current density of 200 $mA{\cdot}cm^{-2}$.

By constructing the backbone structure with different types of aryl-units, the formation of micro-phase separation structures within the anion exchange membrane can be promoted, thereby further improving its performance. Song et al. [53] selected m-terphenyl and p-terphenyl as the skeleton structure and introduced

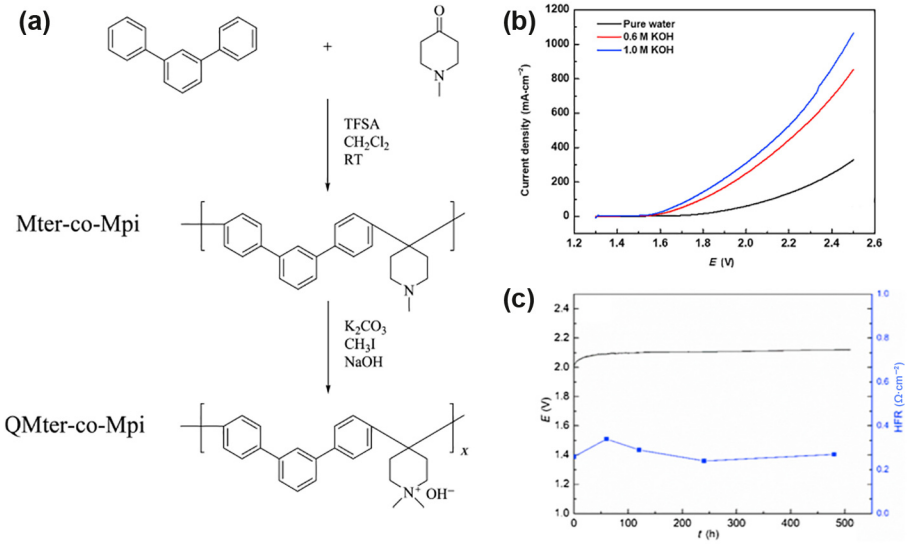

Figure 12 (a) The structure of QMter-co-Mpi AEM. (b) Polarization curves of the AEMWE system based QMter-co-Mpi AEM at different concentrations of electrolyte. (c) Durability test of the QMter-co-Mpi AEM. Reproduced with permission from Ref. [52], © Elsevier B.V. 2020.

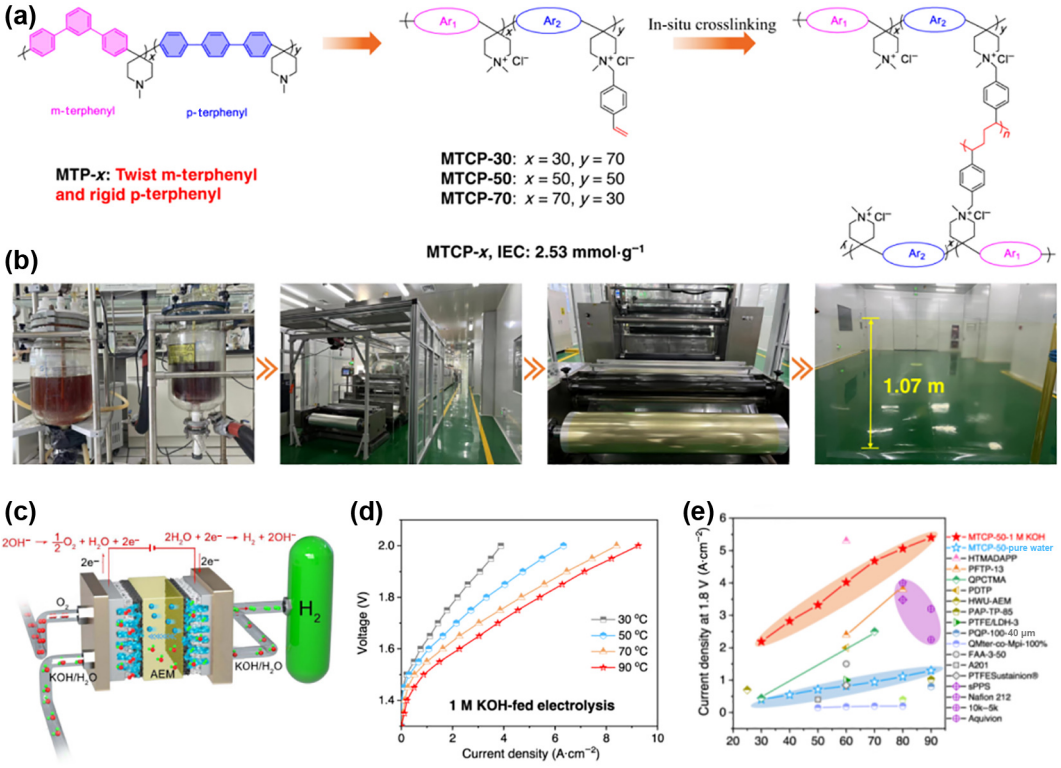

Figure 13 (a) The synthesis process of MTCP-*x* AEMs. (b) The pilot-scale manufacturing of MTCP-50 AEM. (c) Schematic diagram of AEMWE system assembled with the MTCP-50 AEM. (d) Polarization curves of the AEMWE system based MTCP-50 AEM. (e) Performance comparison of current densities at 1.8 V among MTCP-50 and other AEMs. Reproduced with permission from Ref. [53], © Song, W. J. et al. 2023.

4-vinylbenzyl chloride as a cross-linking agent to prepare AEMs named MTCP-*x* (*x* = 70, 50, and 30) (Fig. 13). By adjusting the ratio of the two isomers, MTCP-50 exhibited the highest OH^- conductivity of 217 mS·cm^{-1}@90 °C due to its more ordered morphology. It also showed an excellent alkaline stability (over 8000 h at 80 °C) and mechanical properties (tensile strength: 44.8 MPa, elongation at break: 38.5%). After applying the MTCP-50 for water electrolysis, the current density could reach 5.4 A·cm^{-2} at 1.8 V running at 90 °C, which displayed an advanced level compared with other reported AEMWE performance. Especially, the MTCP-50 membrane with a width > 1 m could be manufactured in a pilot-scale, which was facilitated for the large-scale application of this AEM.

Chen et al. [54] designed an anhydrous cathode water electrolysis device based on poly(fluorene-co-arylpiperidine) (PFAP) AEM and ionomer (Fig. 14). Compared with conventional AEM electrolysis cells, the purity of produced H_2 in the cathode chamber is much higher. However, since water is a reactant in the cathode chamber, but it needs to be captured from the anode chamber, the water diffusion rate of the AEMs also affects the performance of this type of electrolysis cell. In this work, poly(fluorenyl-co-biphenyl piperidinium-14) (PFBP-14) had high IEC and water uptake (350%), which was used as an ionomer on the cathode; poly(fluorenyl-co-terphenyl piperidinium-8) (PFTP-8) had high IEC and low water uptake (80%), which was used as an ionomer on the anode; PFTP-13 AEM had high ionic conductivity (160 mS·cm^{-1}@80 °C) and high water diffusion rate (9.38 × 10^{-8} cm^2·s^{-1}). As a result, the current density could reach 7.68 A·cm^{-2}@2 V under the condition of 80 °C and 1 M KOH electrolyte using precious metals as cathode and anode catalysts, which also surpassed the performance of the state-of-the-art PEM electrolysis cell (6 A·cm^{-2}@2 V). When using non precious metal as cathode and anode catalysts, this electrolysis cell also exhibited excellent water electrolysis performance (1.62 A·cm^{-2}@2 V), and could stably operate for over 1000 h under current density of 0.5 A·cm^{-2}.

Deng et al. [55] constructed a robust polybiphenylpiperidium-based AEMs (tPBPp-*n*-OH) by synergizing the crosslinking process with triazine and the capping procedure with pyridine (Fig. 15). This tPBPp-*n*-OH AEM showed high mechanical strength (79.4 MPa), low swelling ratio (19.2%), excellent alkaline stability (5000 h), and high ionic conductivity (247.2 mS·cm^{-1}). When equipping tPBPp-*n*-OH AEM with commercial Ni-Fe and Ni-Mo catalysts, the electrolyzer could achieve a current density of 3.0 A·cm^{-2}@2 V and a stable operation for 430 h at current density of 1.6 A·cm^{-2}.

To further improve the alkali resistance of the cations, N-methylquinuclidinium cationic group were introduced into the polymer backbone instead of N,N-dimethylpiperidinium. Zeng et al. [56] first proposed N-methylquinuclidinium as a new cationic group and prepared poly(p-terphenyl quinoline) (PPTQ) AEM (Fig. 16). The N-methylquinuclidinium possessed an enhanced alkaline stability compared with the N,N-dimethylpiperidinium, which was induced by reasons of no hydrogen atom at β2-carbon, longer space between α3-carbon and arylene, electron-donating effect of –CH_2CH_2–, and suitable ring structure. As a result, the PPTQ AEM exhibited high OH^- conductivity of 139.1 mS·cm^{-1}@80 °C with no decay even in 10 M NaOH aqueous solution over 1800 h, and high mechanical properties (tensile strength: 41.5 MPa, elongation at break: 50%). After assembled in platinum group metal (PGM)-free water electrolyzer, the current density could reach 1.94 A·cm^{-2} at 2.0 V in 5 M KOH. Meanwhile, PPTQ AEM showed excellent *in-situ* stability after long-term test.

Yin et al. [57] designed a stable AEM with the structure of branched poly(aryl-quinuclidinium) (PAQ-*x*, *x* = 0, 1, 5, and 10) (Fig. 17). Due to the steric hindrance induced by the quinine ring structure, the PAQ-*x* AEMs showed stronger alkaline resistance behaviors compared to that with piperidinium structure. Among

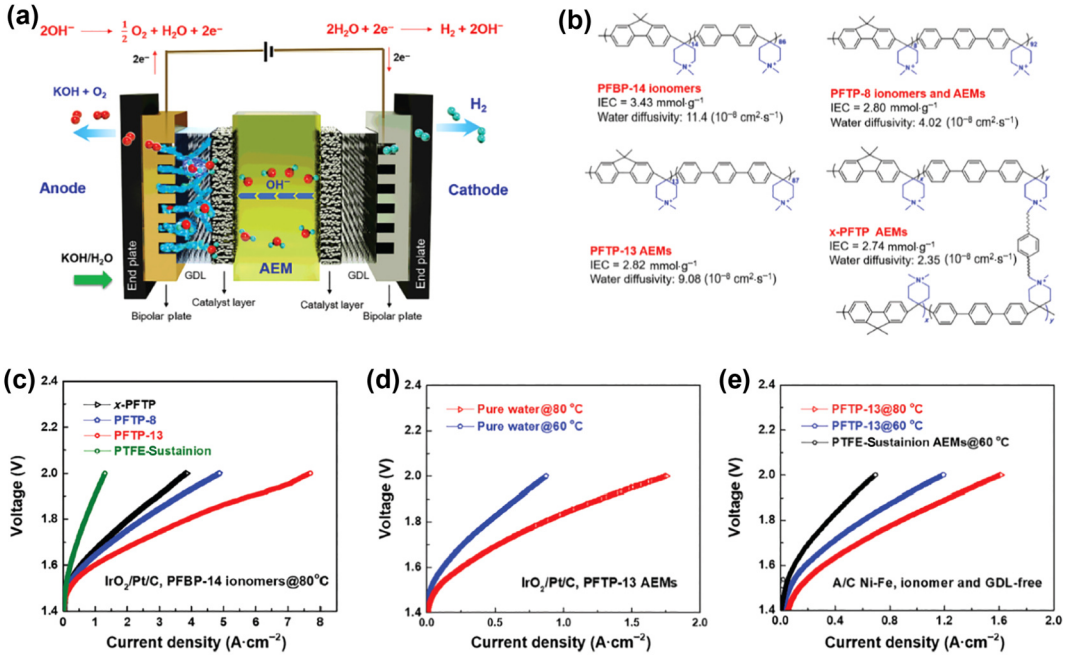

Figure 14 Performance of AEMWE based on PFAP AEM and ionomer. (a) Schematic diagram of anhydrous cathode AEMWE system. (b) Structures of the PFAP AEMs and ionomers. (c) Polarization curves based PFAP AEMs. (d) Polarization curves based PFTP-13 AEM using pure water. (e) Polarization curves based PFTP-13 AEM using non-noble metal catalysts. Reproduced with permission from Ref. [54], © The Royal Society of Chemistry 2021.

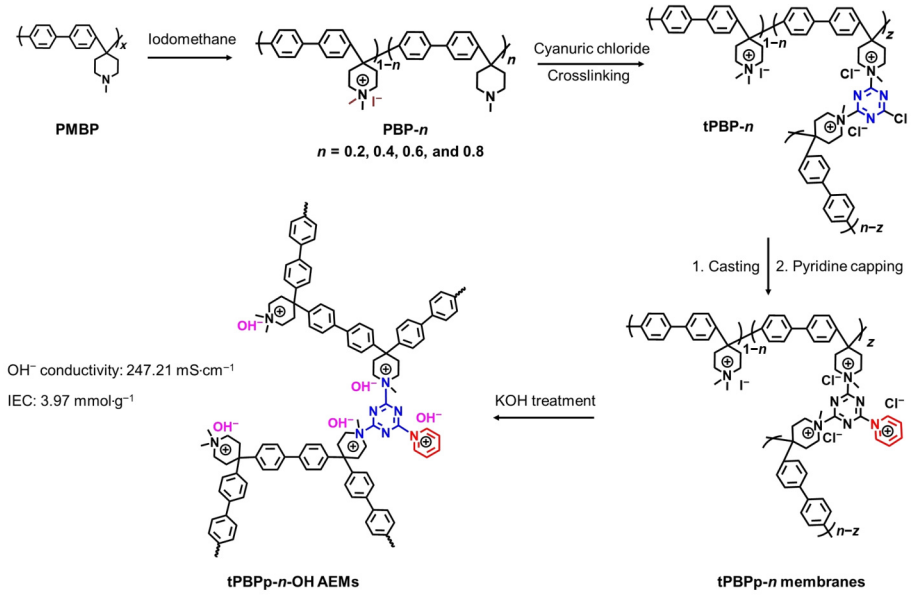

Figure 15 The synthesis of tPBPp-*n*-OH AEMs. Reproduced with permission from Ref. [55], © Wiley-VCH GmbH 2024.

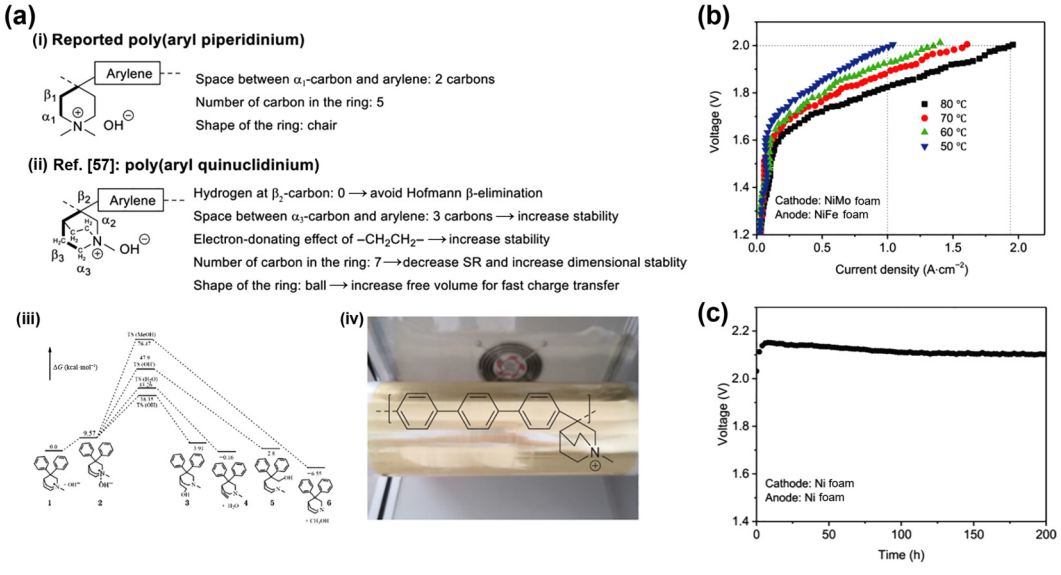

Figure 16 (a) Molecular structure and photo images of PPTQ AEM. (b) Polarization curve of the AEMWE system based PPTQ AEM. (c) Durability test of the AEMWE system based PPTQ AEM. Reproduced with permission from Ref. [56], © Wiley-VCH GmbH 2023.

the series of PAQ-*x*, PAQ-5 exhibited the OH^- conductivity of 186.54 mS·cm^{-1} at 80 °C with excellent dimensional stability (swelling ratio of 6.25%) and alkaline stability (retaining 97% after 2500 h treatment). As a result, the electrical cell using PAQ-5 as the membrane could achieve a high current density of 8 A·cm^{-2} at 2 V and 80 °C, with an excellent stability in a gradient constant current test over 2446 h.

It should be noted that, during the water electrolysis process, the requirements for the stability of AEMs are more stringent compared with those in the static alkaline solution soaking conditions. Hu et al. [58] prepared a series of poly (biphenylpiperidine-co-biphenylindole ketone) (PTP) AEMs (Fig. 18), and the PTP-90 membrane exhibited the highest ionic conductivity (128.9 mS·cm^{-1}@80 °C). The current density of the membrane electrode assembly prepared using PTP-90 membrane could reach 1000 mA·cm^{-2}@2.2 V at 75 °C. In the durability test of the electrolytic cell, the degradation products of cationic groups in PTP-90 could be clearly observed after continuous operation at 55 °C and current density of 400 mA·cm^{-2} for 120 h; while there was no observed degradation process of PTP-90 membrane even after soaking the membrane in 10 M NaOH at 55 °C for 200 h. This result suggested that the working environment of electrolyzers may accelerate the degradation process of AEMs.

To facilitate the comparison of the effects of different anion exchange membranes on the performance of electrolytic water, we summarized the performance of AEMWE using different AEMs in Table 3.

4 Summary and outlook

In summary, AEMs have been widely applied in the fields of hydrogen production through water electrolysis, and the reported performance of AEMs is summarized in Table 3. Although it has been made significant progress in improving the individual

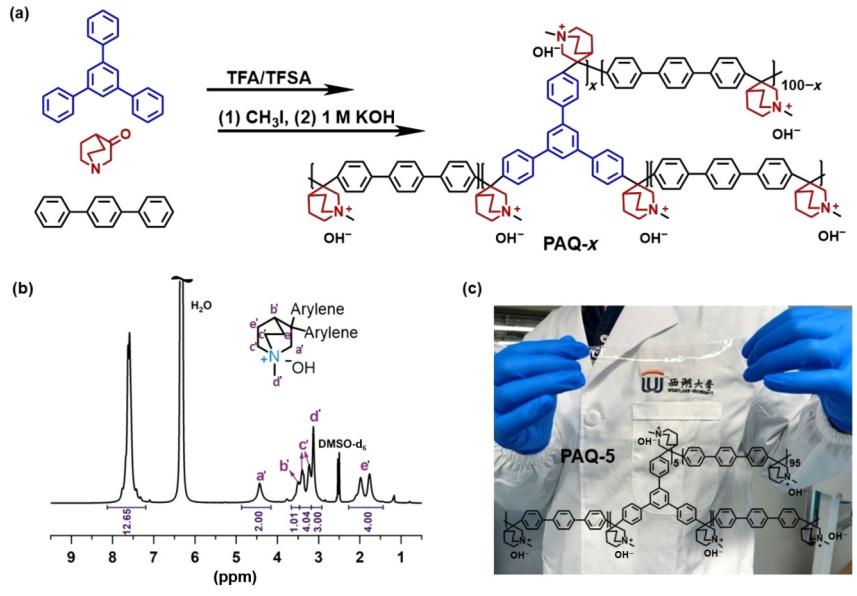

Figure 17 The structure of PAQ-*x* AEMs. Reproduced with permission from Ref. [57], © Wiley-VCH GmbH 2024.

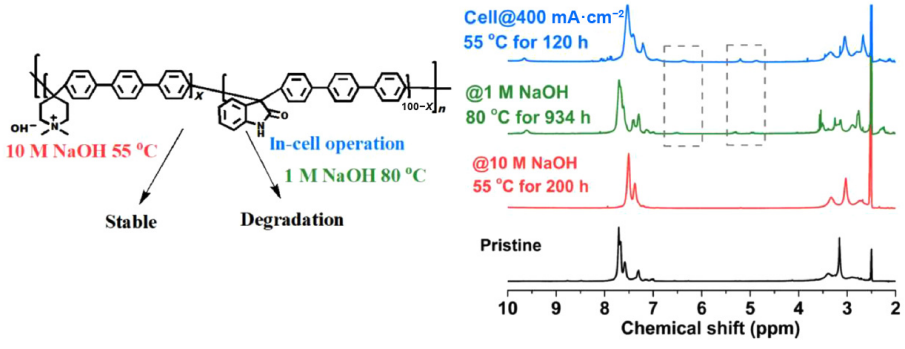

Figure 18 The degradation process of PTP AEMs in the durability test. Reproduced with permission from Ref. [58], © Elsevier B.V. 2020.

Table 3 The performance summary of AEMWE using different AEMs

Skeleton type	AEM	Conductivity (mS·cm^{-1})	Cathode catalyst	Anode catalyst	Electrolyte	AEMWE performance	References
Poly (arylene ether)	xQAPS	—	Ni-Mo	Ni-Fe	Pure water	0.4 A·cm^{-2}@1.8 V, 70 °C	[44]
	PSF-TMA	—	Pt black	Ru-Pb pyrochlore	Pure water	0.4 A·cm^{-2}@1.8 V, 50 °C	[45]
Polyolefin	BMP-c-CMPSF	53.7 (80 °C)	Raney Ni	Ni-Fe	1 M KOH	0.38 A·cm^{-2}@1.8 V, 50°C	[46]
	SEBS-Pi	> 10 (30 °C)	Pt/C	IrO_2	1 M KOH	0.4 A·cm^{-2}@2.0 V, 50 °C	[47]
	PISPVA*x*	89.7 (60 °C)	Pt/C	IrO_2	0.5 M KOH	0.5 A·cm^{-2}@2.0 V, 60 °C	[48]
	BPN1-100	122 (80 °C)	Pt/C	IrO_2	1 M NaOH	0.4 A·cm^{-2}@2.1 V, 50 °C	[49]
	QPC-TMA	154 (80 °C)	Pt/C	IrO_2	1 M KOH	3.5 A·cm^{-2}@1.9 V, 70 °C	[50]
	PFOTFPh-TMA	> 100 (80 °C)	Pt/C	IrO_2	1 M KOH	1 A·cm^{-2}@1.77 V, 80 °C	[51]
Polyaryl	QMter-co-Mpi	66 (80 °C)	Pt/C	IrO_2	1 M KOH	1.064 A·cm^{-2}@2.5 V, 50 °C	[52]
	MTCP-50	217 (90 °C)	Pt/Ru/C	Ni-Fe	1 M KOH	5.4 A·cm^{-2}@1.8 V, 90 °C	[53]
	PFTP-13	160 (80 °C)	Pt/C	IrO_2	1 M KOH	7.68 A·cm^{-2}@2.0 V, 80 °C	[54]
	tPBPp-*n*-OH	247.2 (80 °C)	Ni-Mo	Ni-Fe	1 M KOH	3 A·cm^{-2}@2.0 V, 80 °C	[55]
	PPTQ	139.1 (80 °C)	Ni-Mo	Ni-Fe	5 M KOH	1.94 A·cm^{-2}@2.0 V, 80 °C	[56]
	PAQ-5	186.5 (80 °C)	Ni-Mo	Ni-Fe	1 M KOH	8 A·cm^{-2}@2.0 V, 80 °C	[57]
	PTP-90	128.9 (80 °C)	Pt/C	IrO_2	1 M NaOH	1 A·cm^{-2}@2.2 V, 75 °C	[58]

performance of AEMs, the design and preparation of AEMs with excellent comprehensive performance for industrial application are still facing great challenges. On the one hand, it is difficult to achieve high ionic conductivity and high chemical stability simultaneously, because the alkaline resistance of cationic groups is usually achieved by increasing steric hindrance to reduce the attack of OH^-, which will limit the conductivity rate of OH^-. On the other hand, it is also difficult to achieve high ionic conductivity and high

dimensional stability. In general, the improvement of ionic conductivity is achieved by increasing IEC, but it will lead to increasing the water uptake and swelling ratio. These above two factors limit the application of AEMs in actual water electrolysis process. Therefore, it is necessary to optimize the structure of AEMs, especially with a focus on improving the microphase separation structure, to enhance the ionic conductivity, stability, and mechanical strength simultaneously, which can meet the actual requirements for water electrolysis.

In addition, the existing evaluation standards for the performance of AEMs were inconsistent, especially in the measurement of long-term stability, which limits the comprehensive evaluation for the characteristics of AEMs and the comparisons among various AEMs. Therefore, it is urgent to establish a universally accepted measurement and evaluation technology system to screen out high-performance AEMs for water electrolysis and further efficiently improve the performance of AEMs through structure design. Meanwhile, the intrinsic performance of AEMs can directly affect the core indicators of electrolyzers, such as current density, energy consumption, and dynamic response time. Thus, establishing a comprehensive performance evaluation system of AEMs for actual acquisitions of water electrolysis is also a key link in the industrialization of AEMWE technology.

From a practical application perspective, AEMWE technology has characteristics of high temperature, strict alkaline environment, and gas–liquid mass transfer, which puts forward higher requirements for the promotion and application of AEMs. Therefore, it is necessary to further explore the structure design of AEMs, including the polymerization of ether-free skeletons and the grafting of alkaline resistant cations, and the optimization of membrane preparation processes. Meanwhile, it is crucial to guide the design and development of AEMs through standard and comprehensive application research to promote their industrialization process for the hydrogen production by water electrolysis. Beyond water electrolyzers, AEMs can also be applied in other electrochemical reactors, and the design and synthesis of AEMs tailored for distinct reactor types remains a compelling avenue for future exploration.

Data availability

All data needed to support the conclusions in the paper are presented in the manuscript. Additional data related to this paper may be requested from the corresponding author upon request.

Acknowledgements

This work was financially supported by the China Huaneng Group Found Project (Nos. HNKJ24-H12, HNKJ22-H130, HNKJ21-H07, and HNKJ24-H13) and the Huaneng Clean Energy Research Institute Found Project (Nos. TL-22-CERI01 and CERI/TU-23-CERI03).

Declaration of competing interest

All the contributing authors report no conflict of interests in this work.

Author contribution statement

Q. C. L.: Data curation, writing – original draft, writing – review & editing. X. P. Y.: Data curation, investigation. W. Q. G.: Data curation, investigation. G. S. L.: Funding acquisition, project administration. J. Y. W.: Project administration. N. J.: Supervision. X. L. W.: Supervision. T. B.: Supervision. P. L.: Formal analysis, investigation. J. N. Z.: Investigation. J. W.: Project administration. L. H.: Investigation. T. Y. Z.: Investigation. R. L. H.: Investigation. B. H.: Investigation. K. X. Z.: Investigation. Z. B. R.: Project administration, data curation, writing – review & editing. All the authors have approved the final manuscript.

Use of AI statement

None.

References

[1] Shih, A. J.; Monteiro, M. C. O.; Dattila, F.; Pavesi, D.; Philips, M.; da Silva, A. H. M.; Vos, R. E.; Ojha, K.; Park, S.; van der Heijden, O. et al. Water electrolysis. *Nat. Rev. Methods Primers* **2022**, *2*, 84.

[2] Yang, Y. M.; Shao, Z. G.; Hou, M.; Yi, B. L.; Duan, F. W.; Yu, H. X. Hydrogen production by water electrolysis: Progress and suggestions. *Strategic Study CAE* **2021**, *23*, 146–152.

[3] Xu, S. R.; Wu, Q.; Lu, B. A.; Tang, T.; Zhang, J. N.; Hu, J. S. Recent advances and future prospects on industrial catalysts for green hydrogen production in alkaline media. *Acta Phys.—Chim. Sin.* **2023**, *39*, 2209001.

[4] Zhang, Y. Q.; Cui, W. Z.; Li, L. J.; Wang, C. B.; Zhan, C.; Quan, X. J. Dual-aligned porous electrodes for enhanced hydrogen evolution in alkaline water electrolysis. *Nano Res.* **2024**, *17*, 3835–3843.

[5] Tüysüz, H. Alkaline water electrolysis for green hydrogen production. *Acc. Chem. Res.* **2024**, *57*, 558–567.

[6] Chen, F. Y.; Qiu, C.; Wu, Z. Y.; Wi, T. U.; Finfrock, Y. Z.; Wang, H. T. Ruthenium-lead oxide for acidic oxygen evolution reaction in proton exchange membrane water electrolysis. *Nano Res.* **2024**, *17*, 8671–8677.

[7] Wang, T. Z.; Cao, X. J.; Jiao, L. F. PEM water electrolysis for hydrogen production: Fundamentals, advances, and prospects. *Carbon Neutrality* **2022**, *1*, 21.

[8] Ni, M.; Leung, M. K. H.; Leung, D. Y. C. Technological development of hydrogen production by solid oxide electrolyzer cell (SOEC). *Int. J. Hydrogen Energy* **2008**, *33*, 2337–2354.

[9] Lahrichi, A.; El Issmaeli, Y.; Kalanur, S. S.; Pollet, B. G. Advancements, strategies, and prospects of solid oxide electrolysis cells (SOECs): Towards enhanced performance and large-scale sustainable hydrogen production. *J. Energy Chem.* **2024**, *94*, 688–715.

[10] Li, D. G.; Park, E. J.; Zhu, W. L.; Shi, Q. R.; Zhou, Y.; Tian, H. Y.; Lin, Y. H.; Serov, A.; Zulevi, B.; Baca, E. D. et al. Highly quaternized polystyrene ionomers for high performance anion exchange membrane water electrolysers. *Nat. Energy* **2020**, *5*, 378–385.

[11] Han, Y. J.; Shao, L.; Liu, Y. H.; Li, G. D.; Wang, T. Z.; Zheng, X. R.; Li, J. H.; Han, X. P.; Hu, W. B.; Deng, Y. D. Sulfate-assisted Ni/Fe-based electrodes for anion exchange membrane saline splitting. *Nano Res.* **2024**, *17*, 5985–5995.

[12] Shiva Kumar, S.; Ramakrishna, S. U. B.; Krishna, S. V.; Srilatha, K.; Devi, B. R.; Himabindu, V. Synthesis of titanium(IV) oxide composite membrane for hydrogen production through alkaline water electrolysis. *S. Afr. J. Chem. Eng.* **2018**, *25*, 54–61.

[13] Zeng, K.; Zhang, D. K. Recent progress in alkaline water electrolysis for hydrogen production and applications. *Prog. Energy Combust. Sci.* **2010**, *36*, 307–326.

[14] Aricò, A. S.; Siracusano, S.; Briguglio, N.; Baglio, V.; Di Blasi, A.; Antonucci, V. Polymer electrolyte membrane water electrolysis:

Status of technologies and potential applications in combination with renewable power sources. *J. Appl. Electrochem.* **2012**, *43*, 107–118.

[15] Shiva Kumar, S.; Himabindu, V. Hydrogen production by PEM water electrolysis—A review. *Mater. Sci. Energy Technol.* **2019**, *2*, 442–454.

[16] Hua, K.; Ding, R.; Duan, X.; Rui, Z. Y.; Li, X. K.; Wu, Y. K.; Yang, D. R.; Li, J.; Liu, J. G. Catalytic activity of nanometer-sized Ir–O_x catalysts with different coordination numbers for electrocatalytic oxygen evolution. *ACS Appl. Nano Mater.* **2023**, *7*, 487–497.

[17] Hua, K.; Li, X. K.; Rui, Z. Y.; Duan, X.; Wu, Y. K.; Yang, D. R.; Li, J.; Liu, J. G. Integrating atomically dispersed Ir sites in $MnCo_2O_{4.5}$ for highly stable acidic oxygen evolution reaction. *ACS Catal.* **2024**, *14*, 3712–3724.

[18] Liang, M. D.; Yu, B.; Wen, M. F.; Chen, J.; Xu, J. M.; Zhai, Y. C. Preparation of LSM-YSZ composite powder for anode of solid oxide electrolysis cell and its activation mechanism. *J. Power Sources* **2009**, *190*, 341–345.

[19] Abbasi, R.; Setzler, B. P.; Lin, S. S.; Wang, J. H.; Zhao, Y.; Xu, H.; Pivovar, B.; Tian, B. Y.; Chen, X.; Wu, G. et al. A roadmap to low-cost hydrogen with hydroxide exchange membrane electrolyzers. *Adv. Mater.* **2019**, *31*, 1805876.

[20] Du, N. Y.; Roy, C.; Peach, R.; Turnbull, M.; Thiele, S.; Bock, C. Anion-exchange membrane water electrolyzers. *Chem. Rev.* **2022**, *122*, 11830–11895.

[21] Miller, H. A.; Bouzek, K.; Hnat, J.; Loos, S.; Bernäcker, C. I.; Weißgärber, T.; Röntzsch, L.; Meier-Haack, J. Green hydrogen from anion exchange membrane water electrolysis: A review of recent developments in critical materials and operating conditions. *Sustain. Energy Fuels* **2020**, *4*, 2114–2133.

[22] Shirvanian, P.; Loh, A.; Sluijter, S.; Li, X. H. Novel components in anion exchange membrane water electrolyzers (AEMWE's): Status, challenges and future needs. A mini review. *Electrochem. Commun.* **2021**, *132*, 107140.

[23] Wu, Y.; Luo, J. *In situ* growth of a Pd/Ni$(OH)_2$/NF composite catalyst for the hydrogen evolution reaction. *Acta Phys.—Chim. Sin.* **2016**, *32*, 2745–2752.

[24] Li, M. T.; Zheng, X. Q.; Li, L.; Wei, Z. D. Research progress of hydrogen oxidation and hydrogen evolution reaction mechanism in alkaline media. *Acta Phys.—Chim. Sin.* **2021**, *37*, 2007054.

[25] Wang, H. Q.; Xu, J. H.; Zhang, Q. B.; Hu, S. X.; Zhou, W. J.; Liu, H.; Wang, X. Super-hybrid transition metal sulfide nanoarrays of Co_3S_4 nanosheet/p-doped WS_2 nanosheet/Co_9S_8 nanoparticle with Pt-like activities for robust all-pH hydrogen evolution. *Adv. Funct. Mater.* **2022**, *32*, 2112362.

[26] Chen, N. J.; Lee, Y. M. Anion-conducting polyelectrolytes for energy devices. *Trends Chem.* **2022**, *4*, 236–249.

[27] Qiu, N.; Lu, W.; Wang, H. Q. Manipulating local CO_2/H_2O ratio in electrocatalytic CO_2 reduction toward multi-carbon product. *Rare Met.* **2025**, *44*, 60–80.

[28] Sun, C. Y.; Li, W.; Wang, H. Q. Cascade electrolysis and thermocatalysis: A reliable system for upgrading C1 to C4 hydrocarbons. *Rare Met.* **2024**, *43*, 410–412.

[29] Sun, C. Y.; Li, W.; Wang, K.; Zhou, W. J.; Wang, H. Q. Polyoxometalates-derived nanostructures for electrocatalysis application. *Rare Met.* **2024**, *43*, 1845–1866.

[30] Mu, Y. L.; Chu, F. L.; Wang, B. L.; Huang, T. Z.; Ding, Z. Y.; Ma, D. L.; Liu, F.; Liu, H.; Wang, H. Q. Manipulating crystallographic growth orientation by cation-enhanced gel-polymer electrolytes toward reversible low-temperature zinc-ion batteries. *InfoMat* **2024**, *6*, e12611.

[31] Varcoe, J. R.; Atanassov, P.; Dekel, D. R.; Herring, A. M.; Hickner, M. A.; Kohl, P. A.; Kucernak, A. R.; Mustain, W. E.; Nijmeijer, K.; Scott, K. et al. Anion-exchange membranes in electrochemical energy systems. *Energy Environ. Sci.* **2014**, *7*, 3135–3191.

[32] Hagesteijn, K. F. L.; Jiang, S. X.; Ladewig, B. P. A review of the synthesis and characterization of anion exchange membranes. *J. Mater. Sci.* **2018**, *53*, 11131–11150.

[33] You, W.; Noonan, K. J. T.; Coates, G. W. Alkaline-stable anion exchange membranes: A review of synthetic approaches. *Prog. Polym. Sci.* **2020**, *100*, 101177.

[34] Zakaria, Z.; Kamarudin, S. K. A review of alkaline solid polymer membrane in the application of AEM electrolyzer: Materials and characterization. *Int. J. Energy Res.* **2021**, *45*, 18337–18354.

[35] Gottesfeld, S.; Dekel, D. R.; Page, M.; Bae, C.; Yan, Y. S.; Zelenay, P.; Kim, Y. S. Anion exchange membrane fuel cells: Current status and remaining challenges. *J. Power Sources* **2018**, *375*, 170–184.

[36] Gu, S.; Cai, R.; Yan, Y. S. Self-crosslinking for dimensionally stable and solvent-resistant quaternary phosphonium based hydroxide exchange membranes. *Chem. Commun.* **2011**, *47*, 2856–2858.

[37] Pan, J.; Li, Y.; Zhuang, L.; Lu, J. T. Self-crosslinked alkaline polymer electrolyte exceptionally stable at 90 °C. *Chem. Commun.* **2010**, *46*, 8597–8599.

[38] Zhou, J. F.; Unlu, M.; Vega, J. A.; Kohl, P. A. Anionic polysulfone ionomers and membranes containing fluorenyl groups for anionic fuel cells. *J. Power Sources* **2009**, *190*, 285–292.

[39] Lee, S. A.; Kim, J.; Kwon, K. C.; Park, S. H.; Jang, H. W. Anion exchange membrane water electrolysis for sustainable large-scale hydrogen production. *Carbon Neutralization* **2022**, *1*, 26–48.

[40] Henkensmeier, D.; Najibah, M.; Harms, C.; Žitka, J.; Hnát, J.; Bouzek, K. Overview: State-of-the art commercial membranes for anion exchange membrane water electrolysis. *J. Electrochem. Energy Convers. Storage* **2021**, *18*, 024001.

[41] Marino, M. G.; Kreuer, K. D. Alkaline stability of quaternary ammonium cations for alkaline fuel cell membranes and ionic liquids. *ChemSusChem* **2015**, *8*, 513–523.

[42] Li, H. H.; Yu, N.; Gellrich, F.; Reumert, A. K.; Kraglund, M. R.; Dong, J. H.; Aili, D.; Yang, J. S. Diamine crosslinked anion exchange membranes based on poly(vinyl benzyl methylpyrrolidinium) for alkaline water electrolysis. *J. Membr. Sci.* **2021**, *633*, 119418.

[43] Han, J. J.; Zhu, L.; Pan, J.; Zimudzi, T. J.; Wang, Y.; Peng, Y. Q.; Hickner, M. A.; Zhuang, L. Elastic long-chain multication cross-linked anion exchange membranes. *Macromolecules* **2017**, *50*, 3323–3332.

[44] Xiao, L.; Zhang, S.; Pan, J.; Yang, C. X.; He, M. L.; Zhuang, L.; Lu, J. T. First implementation of alkaline polymer electrolyte water electrolysis working only with pure water. *Energy Environ. Sci.* **2012**, *5*, 7869–7871.

[45] Parrondo, J.; Arges, C. G.; Niedzwiecki, M.; Anderson, E. B.; Ayers, K. E.; Ramani, V. Degradation of anion exchange membranes used for hydrogen production by ultrapure water electrolysis. *RSC Adv.* **2014**, *4*, 9875–9879.

[46] An, E. J.; Sim, G. H.; Yu, S. M.; Kim, H. G.; An, S. J.; Lee, C.; Kim, M.; Kim, J. H.; Lee, J. H.; Chi, W. S. Cross-linked polysulfone membranes with controllable cross-linkers for anion-exchange membrane water electrolysis. *Eur. Polym. J.* **2024**, *221*, 113543.

[47] Su, X. D.; Gao, L.; Hu, L.; Qaisrani, N. A.; Yan, X. M.; Zhang, W. J.; Jiang, X. B.; Ruan, X. H.; He, G. H. Novel piperidinium functionalized anionic membrane for alkaline polymer electrolysis with excellent electrochemical properties. *J. Membr. Sci.* **2019**, *581*, 283–292.

[48] Park, H. J.; Lee, S. Y.; Lee, T. K.; Kim, H. J.; Lee, Y. M. N3-butyl imidazolium-based anion exchange membranes blended with poly(vinyl alcohol) for alkaline water electrolysis. *J. Membr. Sci.* **2020**, *611*, 118355.

[49] Park, E. J.; Capuano, C. B.; Ayers, K. E.; Bae, C. Chemically durable polymer electrolytes for solid-state alkaline water electrolysis. *J. Power Sources* **2018**, *375*, 367–372.

[50] Cha, M. S.; Park, J. E.; Kim, S.; Han, S. H.; Shin, S. H.; Yang, S. H.; Kim, T. H.; Yu, D. M.; So, S.; Hong, Y. T. et al. Poly(carbazole)-based anion-conducting materials with high performance and

durability for energy conversion devices. *Energy Environ. Sci.* **2020**, *13*, 3633–3645.

[51] Soni, R.; Miyanishi, S.; Kuroki, H.; Yamaguchi, T. Pure water solid alkaline water electrolyzer using fully aromatic and high-molecular-weight poly(fluorene-alt-tetrafluorophenylene)-trimethyl ammonium anion exchange membranes and ionomers. *ACS Appl. Energy Mater.* **2021**, *4*, 1053–1058.

[52] Yan, X. M.; Yang, X.; Su, X. D.; Gao, L.; Zhao, J.; Hu, L.; Di, M. T.; Li, T. T.; Ruan, X. H.; He, G. H. Twisted ether-free polymer based alkaline membrane for high-performance water electrolysis. *J. Power Sources* **2020**, *480*, 228805.

[53] Song, W. J.; Peng, K.; Xu, W.; Liu, X.; Zhang, H. Q.; Liang, X.; Ye, B. J.; Zhang, H. J.; Yang, Z. J.; Wu, L. et al. Upscaled production of an ultramicroporous anion-exchange membrane enables long-term operation in electrochemical energy devices. *Nat. Commun.* **2023**, *14*, 2732.

[54] Chen, N. J.; Paek, S. Y.; Lee, J. Y.; Park, J. H.; Lee, S. Y.; Lee, Y. M. High-performance anion exchange membrane water electrolyzers with a current density of 7.68 $A \cdot cm^{-2}$ and a durability of 1000 hours. *Energy Environ. Sci.* **2021**, *14*, 6338–6348.

[55] Deng, G. X.; Liao, Y. W.; Lin, Y. K.; Ding, L.; Wang, H. H. Engineering robust triazine crosslinked and pyridine capped anion exchange membrane for advanced water electrolysis. *Angew. Chem., Int. Ed.* **2024**, *63*, e202412632.

[56] Zeng, M. Y.; He, X. Y.; Wen, J.; Zhang, G. B.; Zhang, H. B.; Feng, H. H.; Qian, Y.; Li, M. N-methylquinuclidinium-based anion exchange membrane with ultrahigh alkaline stability. *Adv. Mater.* **2023**, *35*, 2306675.

[57] Yin, L. Q.; Ren, R.; He, L. L.; Zheng, W. T.; Guo, Y.; Wang, L. Q.; Lee, H.; Du, J.; Li, Z. H.; Tang, T. et al. Stable anion exchange membrane bearing quinuclidinium for high-performance water electrolysis. *Angew. Chem., Int. Ed.* **2024**, *63*, e202400764.

[58] Hu, X.; Huang, Y. D.; Liu, L.; Ju, Q.; Zhou, X. X.; Qiao, X. Q.; Zheng, Z. F.; Li, N. W. Piperidinium functionalized aryl ether-free polyaromatics as anion exchange membrane for water electrolysers: Performance and durability. *J. Membr. Sci.* **2021**, *621*, 118964.